Soft-Tissue Thickness Compensation for Ultrasound Transit Time Spectroscopy Estimated Bone Volume Fraction – an experimental replication study

Ali Hamed Alomari[1,2,3], Marie-Luise Wille[1] and Christian M Langton[1].

[1] Science & Engineering Faculty and Institute of Health & Biomedical Innovation, Queensland University of Technology, Brisbane, QLD, Australia

[2] The University College in Al-Qunfudah, Umm Al-Qura University, Saudi Arabia

E-mail: ali.al-omary@hotmail.com

Abstract

Quantitative Ultrasound (QUS) offers a reliable means to predict osteoporotic fracture risk, although to date it has not been generally used within routine clinical management since it does not provide a direct estimate of bone mineral density (BMD), and hence, the associated WHO criteria for osteopenia and osteoporosis. Langton has proposed that ultrasound propagation through cancellous bone may be considered as an array of parallel sonic-rays, the transit-time of each determined by the corresponding proportion of bone and marrow propagated. This concept has led to the development of ultrasound transit time spectroscopy (UTTS) to estimate solid (bone) volume fraction (SVF). However, within the real-world clinical environment, a bone, such as the calcaneus, has overlying soft-tissues that would result in a significantly time-extended transit time spectrum (TTS), and hence, an underestimated SVF. The aims of this experimental replication study were firstly, to investigate the effect of overlying soft-tissues upon UTTS derived SVF (UTTS-SVF) estimation, and secondly, to develop and evaluate a method to compensate for this, thereby providing a more accurate estimation of SVF. Four 3D-cylindrical replica cancellous bone samples, with flat-parallel cortex discs on opposite faces, were studied; with varying thicknesses of water-replicating overlying soft-tissues. Through-transmission ultrasound signals were recorded, from which the apparent TTS was derived via deconvolution. Pulse-echo signals were utilised to measure the thickness of water overlying the replica cortices. The TTS was then corrected for the ultrasound transit-time associated with the overlying water. Ultrasound transit time spectroscopy derived solid volume fraction (UTTS-SVF) was then calculated, and compared with the SVF value measured with microcomputed tomography (μCT-SVF). The results demonstrated that varying water- thicknesses for each sample provided very similar formats of ultrasound transit-time spectra, but with significant extended time shifts. Compensation for overlying water thickness provided an accurate estimate of SVF for all samples; the overall of agreement between UTTS-SVF with μCT-SVF being 92.68%. It is therefore suggested that UTTS has

the potential to provide a reliable in-vivo estimate of BMD and hence application of the established WHO T-score for routine clinical assessment of osteoporosis.

Keywords: Bone Volume Fraction, Transit Time Spectroscopy, Ultrasound, Soft Tissue

1. Introduction:

A common disease affecting quality of life, particularly for elderly people, is osteoporosis; which refers to "a decrease in bone mass and architectural deterioration of bone tissue, leading to enhanced bone fragility and consequent increase in fracture risk" (Christiansen 1991). Dual energy X-ray absorptiometry (DXA) is generally considered to be the preferred technique for routine clinical assessment of osteoporosis, utilising two X-ray energies; their intensities, along with knowledge of the attenuation coefficients of bone and soft tissue, are used to calculate the areal bone mineral density (aBMD, g/cm^2).

The quantitative ultrasound (QUS) technique has been demonstrated to provide a reliable prediction of osteoporotic fracture risk (Hans *et al* 1996, Bauer *et al* 1997, Thompson *et al* 1998, Njeh *et al* 2000, Moayyeri *et al* 2012); being simpler to use, free from ionising radiation, lower cost and portable compared to DXA. The most common QUS parameters are speed of sound (SOS, m/s), broadband ultrasound attenuation (BUA, dB MHz^{-1}) and stiffness index (SI, %). The correlations of these parameters with both bone volume fraction (BVF) and bone mineral density (BMD) have been extensively investigated (Gonnelli *et al* 1995, Gonnelli *et al* 1996, Hadji *et al* 1999, Karlsson *et al* 2001, Cortet *et al* 2004).

A number of in-vitro studies have reported correlation coefficients of approximately 0.8 between QUS parameters with BVF derived by microcomputed tomography (μCT) in cancellous (trabecular) bone samples; for example, r = 0.79 and 0.84 for SOS and nBUA respectively (Lee 2013) and r = 0.81 and r=0.83 for SOS and nBUA respectively (Padilla *et al* 2008); noting that nBUA (dB MHz^{-1} cm^{-1}) describes BUA divided by sample thickness.

In-vitro studies have reported a broad range of correlation coefficients between BUA and bone density ranging from r = 0.83 to r = 0.97 (McKelvie *et al* 1989; McCloskey *et al* 1990; Nicholson *et al* 1994). It has been suggested that the correlation coefficient variability may be attributed to assessment of tissue samples from differing species (animal and human), and from different anatomical locations. In-vivo correlation coefficients between calcaneal BUA and DXA-estimated BMD range from 0.32 to 0.87 (Njeh *et al* 1997); again, being highly dependent on the anatomical

measurement site. For example, a site-matched calcaneal correlation coefficient of 0.79 has been reported at the calcaneus (Langton and Langton 2000), being only 0.47 for calcaneal BUA and lumbar spine BMD (Prins *et al* 1998).

Significant correlation coefficients have been recorded between SOS and bone density in in-vitro studies ranging between r=0.71 to r=0.93 (; Evans and Tavakoli 1990, Bouxsein *et al* 1995, Njeh *et al* 1995 Barkmann *et al* 2007), while, in-vivo studies have reported lower correlation coefficient varying widely from r=0.34 to 0.72 (Njeh *et al* 1997).

The mathematical combination of BUA and SOS provides further QUS parameters such as stiffness index (SI) [defined as (0.67 x BUA) + (0.28 x SoS) – 420] (Jaworski *et al* 1995) and quantitative ultrasound index (QUI) [defined as 0.41 x (BUA + SOS) – 571] (Magkos *et al* 2005). Number of studies found that stiffness has better correlation with BMD than BUA and SOS alone (Lees et al 1993; Xu et al 2014). However, again, the correlation is dependent on the measurement site. For example, Greenspan et al (1997) found the correlation between SI and BMD is higher in cancellous bone (r=0.86) compared to that in the trochanter, femoral neck and spine, being r= 0.77, r=0.80 and r=0.68 respectively.

QUS is not generally utilised within routine clinical management of osteoporosis since its parameters have not been able to date to provide an accurate estimation of BMD, and hence, assign WHO criteria for osteopenia and osteoporosis to an individual subject.

In 2011, Langton proposed a new concept to describe ultrasound propagation through cancellous bone; considering an array of parallel sonic-rays, the transit time (TT) of each determined by the proportion of bone and marrow propagated, exhibiting maximum TT through entire marrow (t_{max}) and minimum (t_{min}) TT through entire bone (Langton 2011). Thus, a transit time spectrum (TTS) may be described as the proportion $P(t_i)$ of sonic-rays having a particular TT t(i) (Langton and Wille 2013). Since the ultrasound 'output' signal having propagated through a test sample may be described as the mathematical convolution of the 'input' ultrasound signal and the transit time spectrum of the test sample, a TTS may be derived by deconvoluting the 'output' and 'input' ultrasound signals, as illustrated in figure 1.

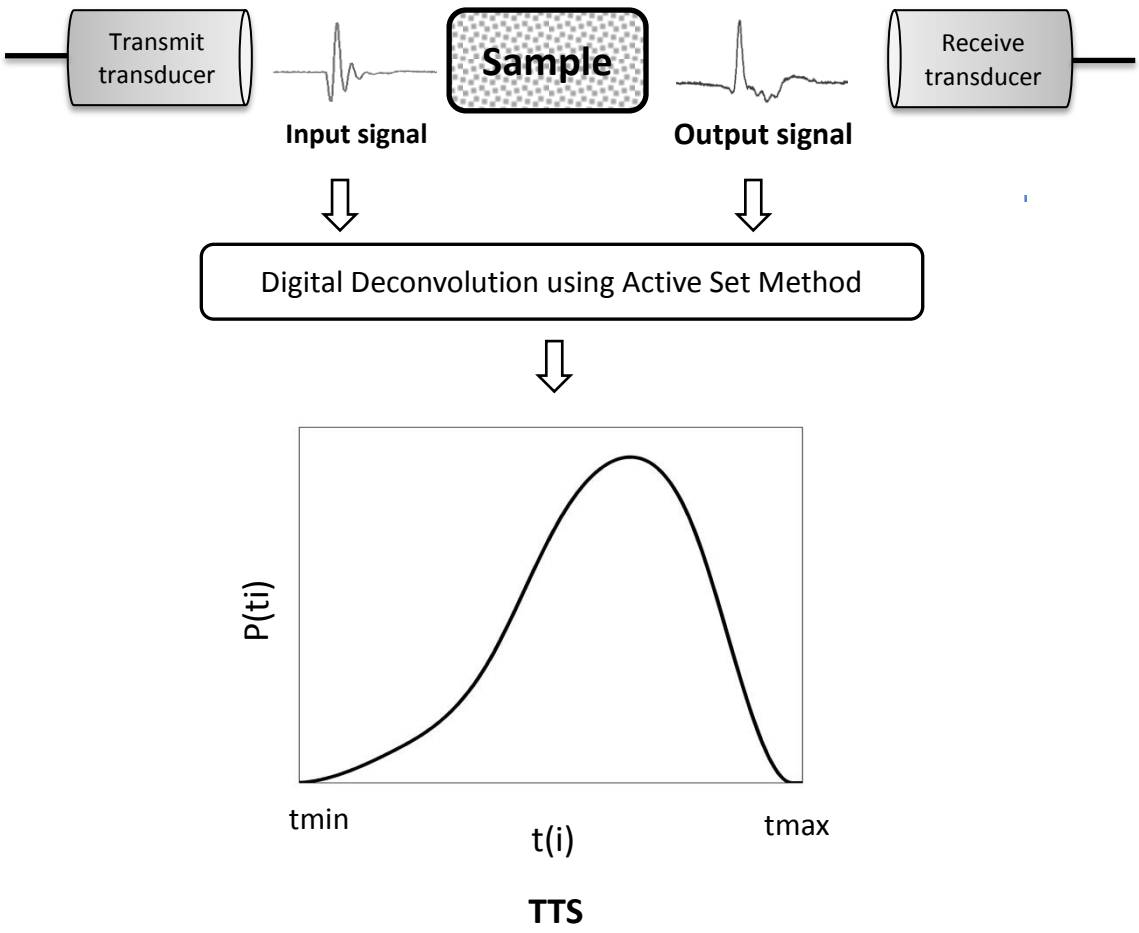

Figure 1. The derivation of an ultrasound transit time spectrum (TTS) via deconvolution.

This concept has led to the development of ultrasound transit time spectroscopy (UTTS) that has been scientifically validated by several studies (Langton *et al* 2014; Wille *et al* 2016; Al-Qahtani and Langton 2016a, 2016b). Recently, Wille and Langton (2016) have reported an accurate estimation of solid volume fraction (SVF). For a solid-liquid composite sample, the transit-time of a particular sonic-ray is determined by the proportion of solid to liquid ($SP(t_i)$), as shown in equation (1). By summing the product of the solid proportion and proportion of sonic-rays at each transit time between t_{min} and t_{max}, we may estimate the overall solid volume fraction of the test sample, as described in equation (2).

$$SP\ (t_i) = 1 - \left[\frac{t_i - t_{min}}{t_{max} - t_{min}}\right] \qquad (1)$$

$$SVF = \sum_{t_i=t_{min}}^{t_i=t_{max}} SP(t_i)\cdot P(t_i) \qquad (2)$$

However, for in-vivo measurement of a bone such as the calcaneus within the heel, there are overlying soft-tissues between the surfaces of the skin and bone. Several studies have demonstrated the effect of overlying soft tissue upon ultrasound measurements. Kotzki et al. examined the influence of soft tissue using four fresh cadaver heels, and recorded an increase of SOS results (+11 to +28 m s^{-1}) after removal of soft tissues, whereas no significant change on BUA measurement was observed (Kotzki *et al* 1994). Häusler et al. (1997) using both contact and water bath methods reported that SOS is sensitive to the presence of soft tissue while BUA is insensitive. Johansen and Stone (1997) have studied the effect of ankle oedema on BUA and SOS. Eleven elderly patients (with average ages of 81 years) with below-knee pitting oedema were assessed. They compared the measurements of the ankle BUA with oedema present to those after removal of oedema. The results showed that oedema reduced the mean of BUA measurements by 14.20%, and the mean SOS by 1.40%.

From an UTTS perspective, the effect of the overlying soft-tissues will introduce a time-delay within the transit time spectrum (figure 2) and will consequently significantly underestimate the SVF.

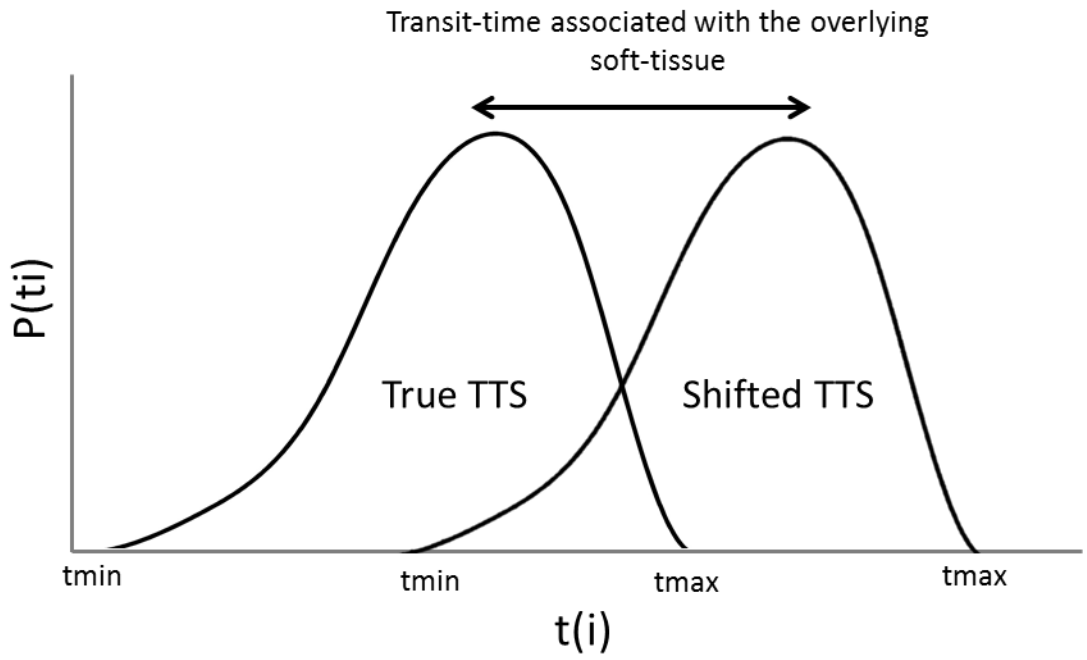

Figure 2. The effect of overlying soft tissue upon TTS.

The aims of this experimental replication study were firstly, to investigate the effect of overlying soft tissues upon UTTS-derived SVF estimation, and secondly, to develop and evaluate a means to compensate for this, thereby providing an accurate estimation of SVF.

2. Materials and Methods:

2.1. Samples:

Four cylindrical (19 mm diameter, 30 mm height) cancellous bone replicating samples with 1 mm flat cortex discs on opposite faces were designed, as shown in figure 3, and 3D-printed using VisiJet FTX material (ProJet1200 Micro-SLA system). The velocity, density and attenuation coefficient of the material were measured as 2470±10 m s^{-1}, 1175 kg m^{-3} and 43±0.4 Np m^{-1} respectively.

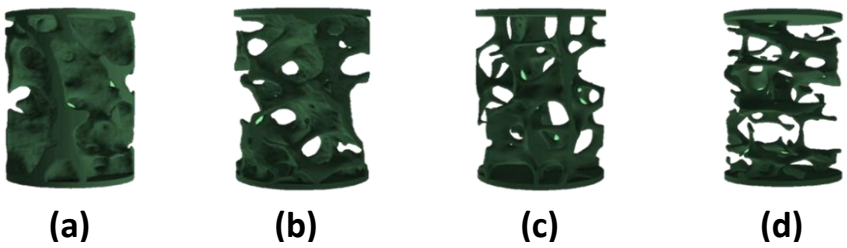

Figure 3. Cancellous bone replicating samples: (a) femoral head (b) iliac crest (c) lumber spine (d) calcaneus.

2.2. Experimental set-up:

Two 19 mm (3/4”), 1 MHz, broadband, planar ultrasound transducers (Harisonics I7-0112-G, Olympus NDT, Waltham, MA, USA), as utilised clinically, were placed coaxially in a water-tank. The transmitting transducer was connected to a spike generator (Panametrics PR5058 pulser-receiver), and the receive transducer was connected to a 14-bit digitiser card operating at a 50-MHz digitisation rate (National Instruments PCI5122, Austin, TX, USA); 5000 data points were collected equating to 100 μs.

The transducer separation was adjusted to replicate varying overlying soft-tissue thicknesses of 5, 10, 15 and 20 mm on either side of the sample. Figure 4 illustrates the experimental set-up demonstrating the position of the replica bone sample and replica soft tissues.

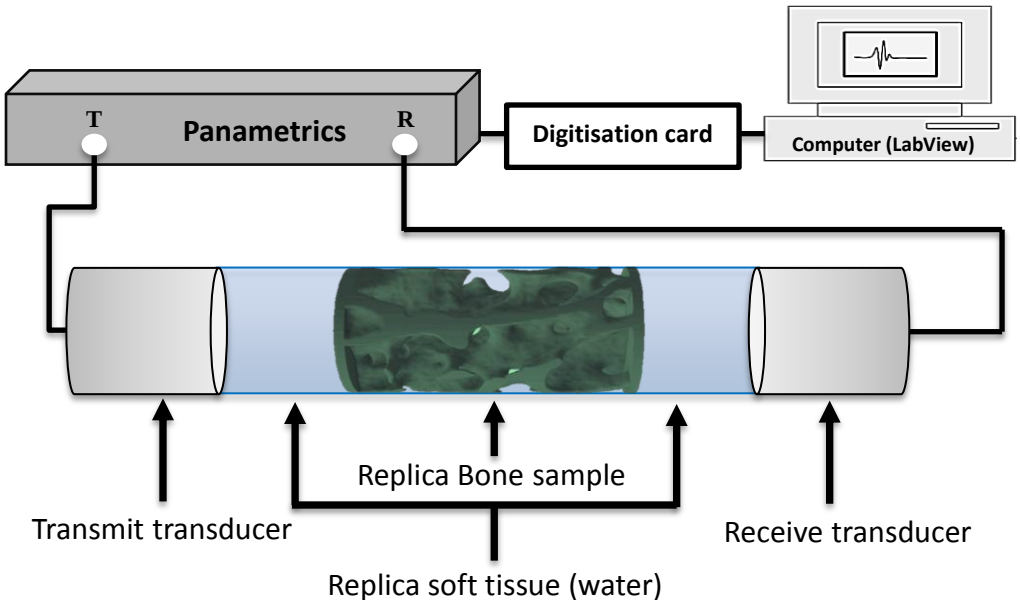

Figure 4. Schematic diagram of experimental set-up.

2.3. Ultrasound measurement and soft tissue thickness correction:

For each sample and a fixed water thickness, through-transmission ultrasound signals through water alone ('input') and through the sample/water ('output') were recorded for UTTS analysis. The procedure was repeated for different water thicknesses. Further, each measurement was repeated five times, the sample being repositioned between measurements.

Pulse-echo signals were measured to estimate the thickness of the water between transducer and sample as [$d = (t/2)/v_w$]; where v_w is the ultrasound velocity through water, measured experimentally at temperatures ranging between 22.4 °C to 23.2 °C and equating to velocities ranging between 1489 m s^{-1} to 1492 m s^{-1}.

Minimum (t_{min}) and maximum (t_{max}) TT were experimentally measured through a fully solid sample of VisiJet FTX material and water respectively as d/v_s and d/v_w respectively, where d is the sample thickness.

The pulser-receiver attenuator settings for the samples ('output', dB_2) ranged between 15 dB and 35 dB, to maximise the signal amplitude before saturation, while the attenuator setting for water alone ('input', dB_1) was 55 dB. Reducing the attenuator setting increases the 'output' signal amplitude that hence increases the apparent proportion of sonic-rays within the deconvolution-derived transit time spectrum ($P(t_i)$). A pulser-receiver attenuator correction was therefore developed and applied to the

deconvolution-derived transit time spectrum, described by equation (3), where ΔdB is the attenuator settings difference (dB) between 'input' and 'output' signal recordings.

$$\textbf{Corrected output signal} = (\textbf{output signal})/\textbf{10\^{}}(\boldsymbol{\Delta dB}\ /\ \textbf{20}) \qquad \textbf{(3)}$$

The 'raw' transit time spectrum (TTS) was derived via deconvolution of the experimental measured 'input' and 'output' ultrasound signals, from which the 'raw' UTTS–SVF was calculated utilising equations 1 and 2.

By definition, the sum of all proportions of sonic-rays ($P(t_i)$) should be unity. However, in practice, this summation is generally slightly reduced, attributed to additional attenuation factors including reflections and scattering within the test sample. The 'raw' TTS was therefore corrected by normalizing the sum of $P(t_i)$ between t_{min} and t_{max} to unity, as illustrated in figure 5. This is primarily based on the assumption that all ultrasound propagated signals would be detected in the absence of wave degradation effects such as phase interference and absorption.

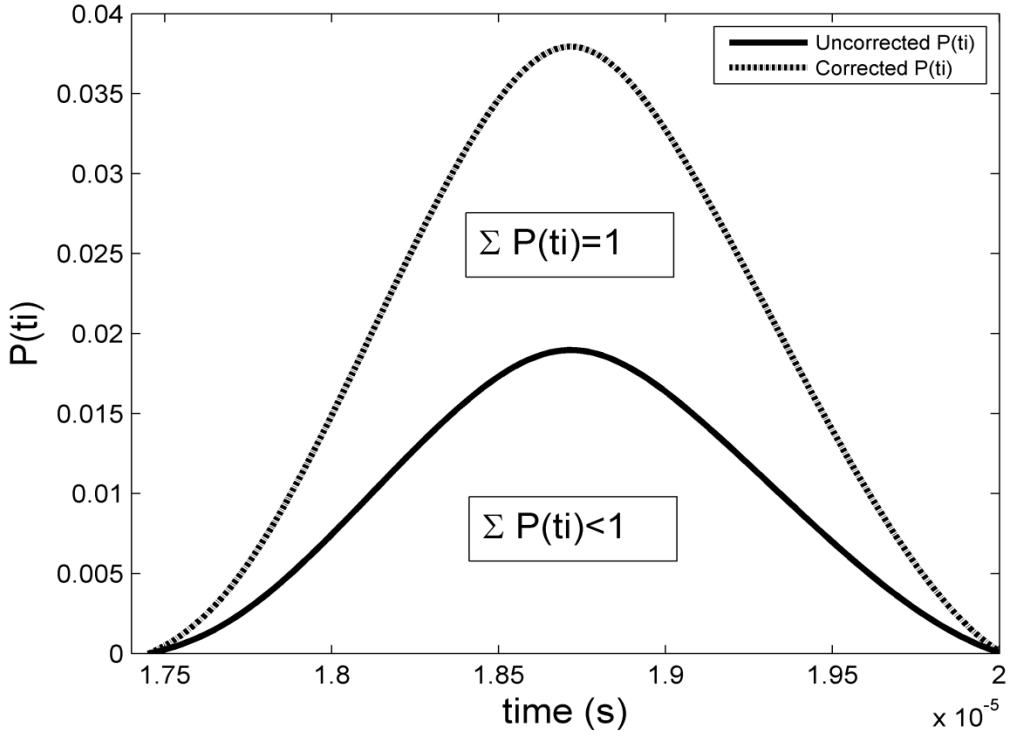

Figure 5: Mechanism of $P(t_i)$ correction.

Finally, the 'raw' TT spectra were corrected for a specific overlying water thickness, achieved by subtracting the corresponding pulse-echo TT measurement.

Applying these two corrections ($P(t_i)$ and overlying soft tissue thickness) provided a corrected TTS, from which corrected UTTS–SVF was derived. UTTS-SVF with and without corrections were then compared to the actual SVF value measured with µCT (µCT-SVF).

Figure 6 shows a detailed flow chart describing the UTTS-SVF derivation process.

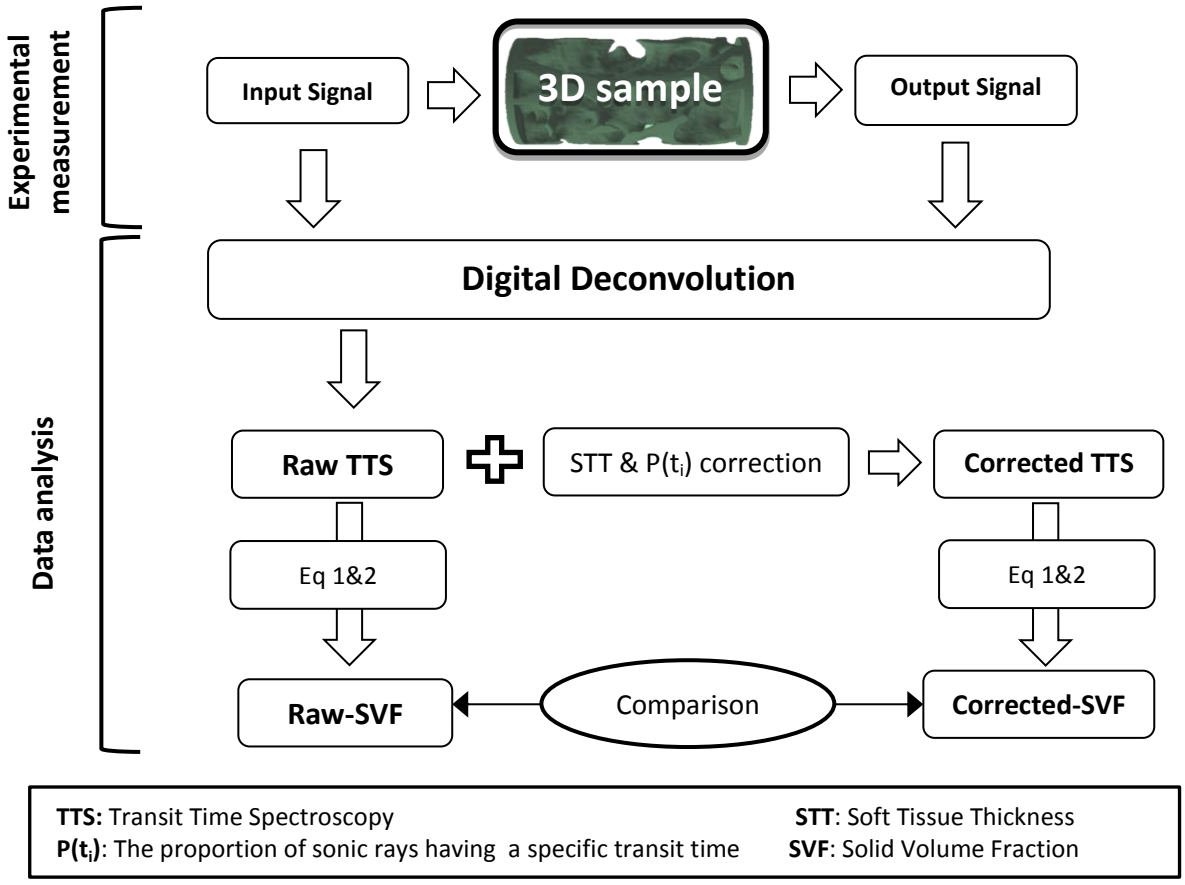

Figure 6. A flow chart describing raw and corrected UTTS-SVF derivation process.

2.4. Micro-Computed Tomography analysis:

The SVF of the replica models was also determined using micro-CT (μCT 40, Scanco Medical, Brütisellen, Switzerland). The samples were scanned in air at 45 kVp and 177 µA, with an isotropic voxel size of 30 μm^3 and a sample time of 0.6 s. The grey scale images were evaluated by applying a region of interest corresponding to the diameter of the cortex disk for each scan slice. The lower threshold of 42 (min/max: 0/1000) was chosen by histogram analysis to separate the trabecular structure from the background. Due to the low x-ray absorbing nature of the polymer, the built in Gaussian filter was adjusted (sigma = 2.3, support = 5) to remove additional noise (Campbell and Sophocleous 2014). The scan and analysis settings were kept constant for all models. The 3D reconstruction and the SVF [%] of each model were then calculated with SCANCO's proprietary

algorithms based on the methods of Hildebrand and Ruegsegger (Hildebrand and Rüegsegger 1997, Hildebrand *et al* 1999). Reconstructed 3D micro-CT images of the utilised samples are shown in table 1.

Table 1. 3D image reconstruction of the micro-CT scans of the four replica models and micro-CT derived SVF.

Sample	FH	IC	LS	CA
	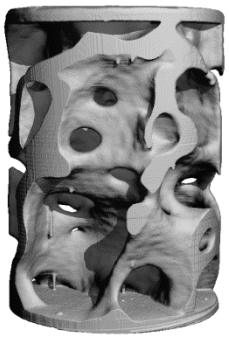	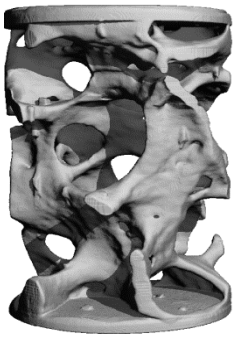	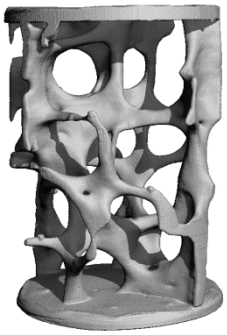	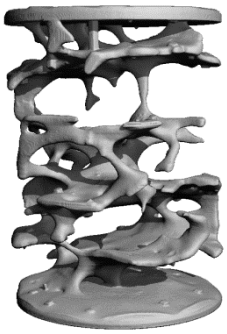
SVF [%]	32.58	22.75	17.49	17.79

2.5. Statistics analysis:

The percentage of agreement between UTTS-SVF and μCT-SVF was performed using Excel 2010 (Microsoft). One-way analysis of variance (one way ANOVA) statistically evaluated the differences between corrected UTTS-SVF measurements at all soft tissue thicknesses for all samples.

3. Results and Discussion:

Plots in figure 7 show qualitative comparisons of TTS for the four replica cancellous bone samples before and after compensation for the ultrasound TT associated with varied water thickness replicating overlying soft-tissue thicknesses.

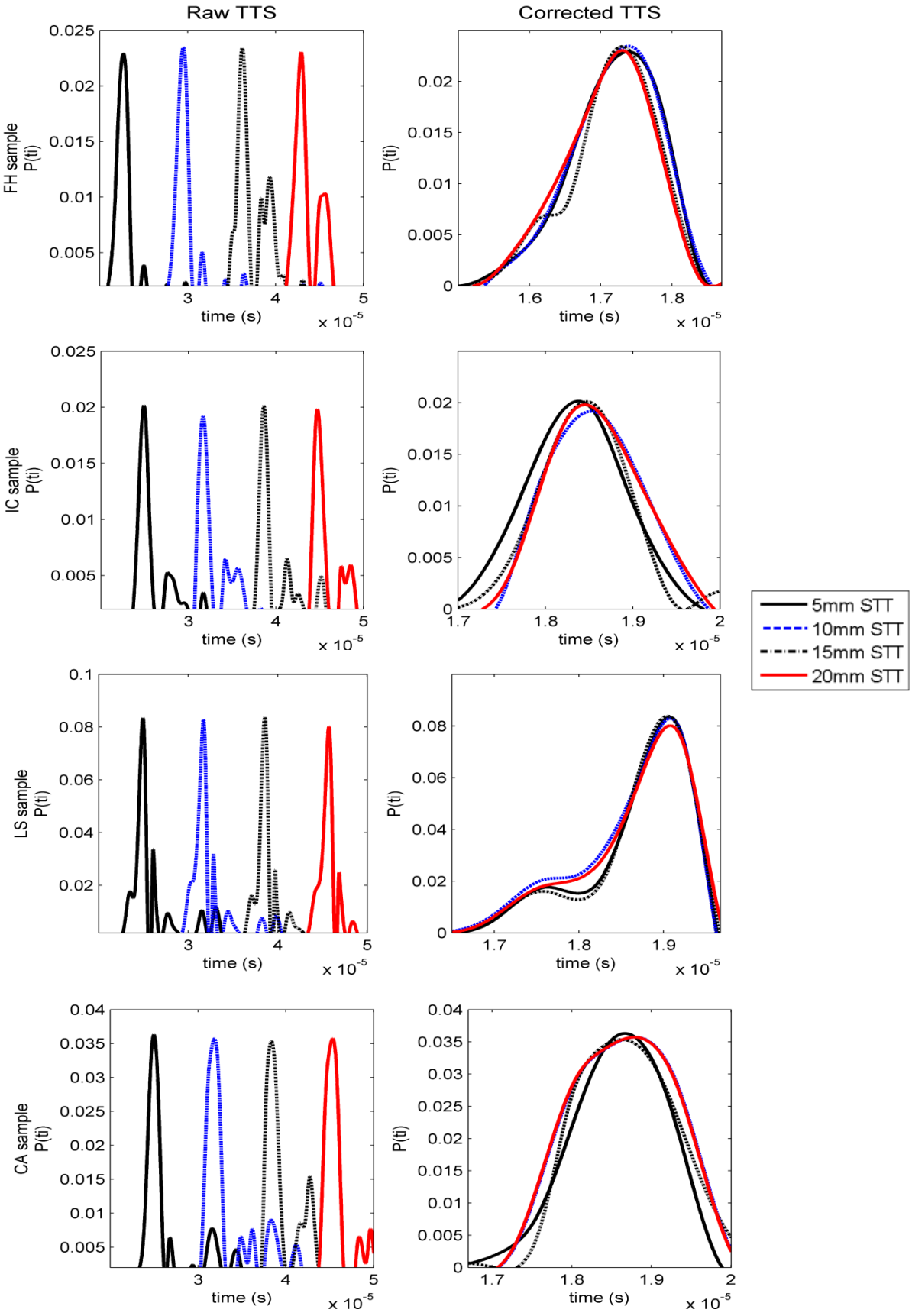

Figure 7. Transit time spectra before (left columns) and after (right columns) compensation for soft tissue thicknesses for the femoral head (FH), iliac crest (IC), lumbar spine (LS), and calcaneus sample (CA) (from top to bottom).

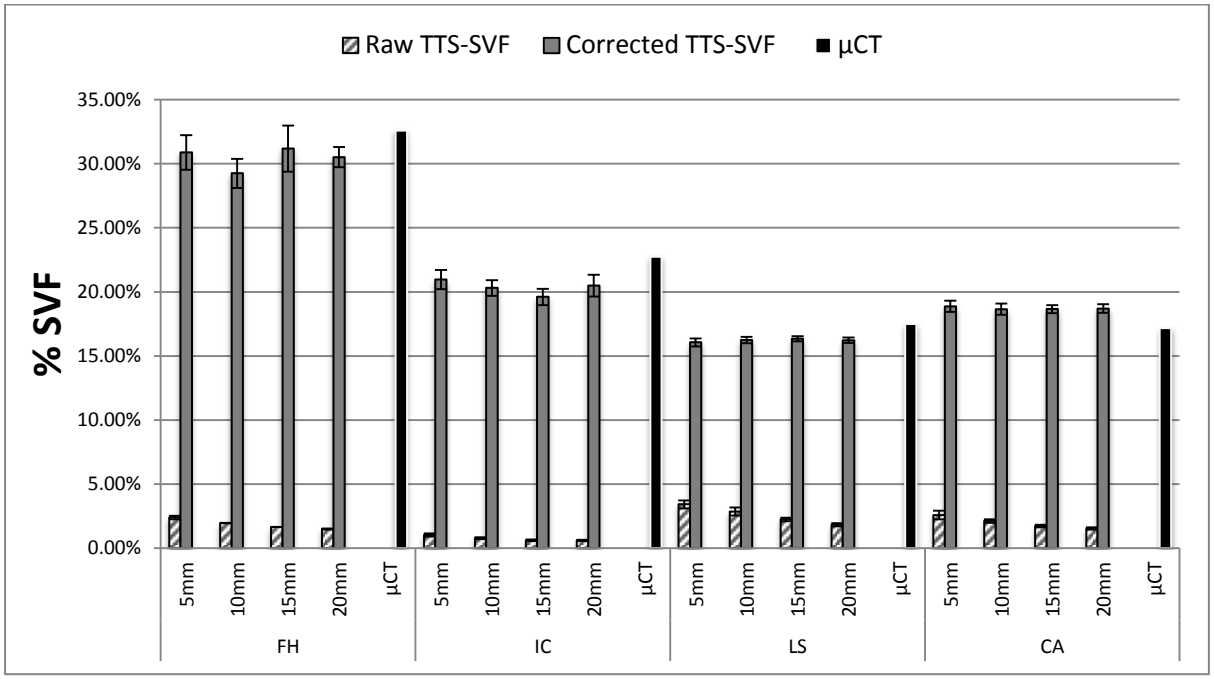

Figure 8. Quantitative comparisons between UTTS-SVF (raw (striped bars) and corrected (grey bars)) and µCT-SVF (black bars) for the four cancellous bone replica models.

Table 2. Average of % agreement of raw and corrected UTTS-SVF with µCT-SVF for all samples demonstrating the level of improvement resulting from mentioned corrections.

	5 mm	10 mm	15 mm	20 mm	Overall average
Raw UTTS-SVF	11.56±6.83 %	9.42±5.84 %	7.57±4.56 %	6.58±3.59 %	8.76 %
Corrected UTTS-SVF	93.24±1.49 %	91.83±2.86 %	92.67±4.44 %	92.93±2.13 %	92.68 %
% improvement	87.44 %	89.53 %	91.66 %	92.77 %	90.35 %

The qualitative comparisons in figure 7 clearly indicate that varying the water thickness for each sample provided very similar formats of TTS, but with overall time shifts commensurate with the corresponding water thickness (figure 7-left columns). Subtraction of the pulse-echo derived transit time provided almost identical TT spectra (figure 7-right columns). These findings agree with the previous study by Häusler which stated that the overlying soft tissue influences SOS (TT shift) but not BUA (same TTS format) (Häusler *et al* 1997).

The overall percentage of agreement between 'raw' UTTS-SVF and µCT-SVF was low, being 8.76%, that increased to 92.68% when soft-tissue thickness and $P(t_i)$ corrected factors were implemented; enhancing the accuracy of measured UTTS-SVF by an average of 90.35% as shown in table 2 and figure 8.

Statistically, there were no significant differences among corrected UTTS-SVF measurements at all water thicknesses for all samples ($p = 0.99$). Further, the results show that corrected UTTS-SVF provided an accurate estimate of μCT-SVF.

Although very good results have been achieved, the study poses some limitations. The measurement of t_{min}, which is the TT solely through bone, might be more difficult when utilizing natural bone tissue samples, compared to the current study, where t_{min} was experimentally measured using a reference block sample. This might be solved through the knowledge of ultrasound velocity through the bone along with the thickness of the examined cancellous bone, which can be determined by subtracting the transducer separation from the entire soft tissue thickness. Further, water was used as a surrogate for all soft-tissues that would be present in-vivo.

The use of replica phantoms provides a controllable environment to investigate the characteristics of ultrasound propagation through human cancellous bone. Several previous studies have mimicked cancellous bone using different phantoms having different material properties such as acrylic (Langton and Wille 2013), stereolithography resin (Aygün et al 2010, Langton 2011), mixture of epoxy resin and gelatine (Clarke et al 1994), polyacetal cuboid (Lee and Choi 2007) and nylon wires (Wear 2009a, 2009b). In this study, we have used VisiJet FTX material with an ultrasound velocity of 2470 m s^{-1} that was lower than that for human bone tissue (2900 m s^{-1}) (Kaufman et al 2007); however, it is still significantly higher than for marrow-replicating water. Hence, a comparable acoustic impedance mismatch exists, resulting in reflection coefficients of 0.32 and 0.53 for VisiJet FTX /water and bone/marrow respectively.

Material absorption and attenuation have been studied extensively as important factors affecting ultrasound propagation through complex structures such as cancellous bone (Le 1998, Wear 2000, Wear 2009a, Zhang *et al* 2011). In this study, we assume these factors are incorporated within the TTS and that material absorption and attenuation are compensated for by applying the $P(t_i)$ correction. Future work will consider the role of absorption and attenuation within the UTTS analysis and it is expected that a better understanding may enhance the ability of UTTS to estimate SVF even more accurately. Furthermore, it is envisaged to extend this work to estimate UTTS-BVF in-vivo, from which the discriminatory abilities of bone status using UTTS and DXA might be compared.

4. Conclusion

This study investigated the ability of UTTS to estimate the SVF of four replica cancellous bone samples, particularly associated with varying overlying soft thickness, replicated using water. Corrected UTTS-SVF provided a percentage of agreement of 92.68%, compared to only 8.76% for

uncorrected UTTS-SVF against ‘gold-standard’ micro-CT derived solid volume fraction (μCT-SVF). UTTS therefore has potential to provide an accurate estimate of BVF in-vivo, thereby offering for the first time, accurate estimation of BMD and implementation of WHO T-score criteria using ultrasound for routine clinical management of osteoporosis.

References

Al-Qahtani S M and Langton C M 2016a Estimation of liquid volume fraction using ultrasound transit time spectroscopy Measurement Science and Technology **27** 125003

Al-Qahtani S M and Langton C M 2016b Ultrasound temporal-spatial phase-interference in complex composite media; a comparison of experimental measurement and simulation prediction *Ultrasonics* **71** 115-26

Aygün H, Attenborough K, Lauriks W and Langton C M 2010 Ultrasonic wave propagation in stereo-lithographical bone replicas *J. Acoust. Soc. Am.* **127** 3781-9

Barkmann R, Laugier P, Moser U, Dencks S, Padilla F, Haiat G, Heller M and Glüer C C 2007 A method for the estimation of femoral bone mineral density from variables of ultrasound transmission through the human femur *Bone* **40** 37-44

Bauer D C, Glüer C C, Cauley J A, Vogt T M, Ensrud K E, Genant H K and Black D M 1997 Broadband ultrasound attenuation predicts fractures strongly and independently of densitometry in older women: a prospective study *Arch. Intern. Med.* **157** 629-34

Bouxsein M L, Radloff S E and Hayes W C 1995 Quantitative ultrasound of the calcaneus reflects trabecular bone strength, modulus, and morphology J. Bone Miner. Res. **10** S175-S

Campbell G M and Sophocleous A 2014 Quantitative analysis of bone and soft tissue by micro-computed tomography: applications to ex vivo and in vivo studies *BoneKEy reports* **3** 564

Christiansen C 1991 Consensus development conference: prophylaxis and treatment of osteoporosis *The American Journal of Medicine* **90** 107-10

Clarke A J, Evans J A, Truscott J G, Milner R and Smith M A 1994 A phantom for quantitative ultrasound of trabecular bone *Phys. Med. Biol.* **39** 1677-87

Cortet B, Boutry N, Dubois P, Legroux-Gérot I, Cotten A and Marchandise X 2004 Does Quantitative Ultrasound of Bone Reflect More Bone Mineral Density Than Bone Microarchitecture? *Calcif. Tissue Int.* **74** 60-7

Evans J A and Tavakoli M B 1990 Ultrasonic attenuation and velocity in bone *Phys. Med. Biol.* **35** 1387-96

Gonnelli S, Cepollaro C, Agnusdei D, Palmieri R, Rossi S and Gennari C 1995 Diagnostic value of ultrasound analysis and bone densitometry as predictors of vertebral deformity in postmenopausal women *Osteoporosis Int.* **5** 413-8

Gonnelli S, Cepollaro C, Pondrelli C, Martini S, Rossi S and Gennari C 1996 Ultrasound parameters in osteoporotic patients treated with salmon calcitonin: A longitudinal study *Osteoporosis Int.* **6** 303-7

Greenspan S L, Bouxsein M L, Melton M E, Kolodny A H, Clair J H, Delucca P T, Stek Jr M, Faulkner K G and Orwoll E S 1997 Precision and Discriminatory Ability of Calcaneal Bone Assessment Technologies *J. Bone Miner. Res.* **12** 1303-13

Hadji P, Hars O, Wüster C, Bock K, Alberts U S, Bohnet H G, Emons G and Schulz K D 1999 Stiffness index identifies patients with osteoporotic fractures better than ultrasound velocity or attenuation alone *Maturitas* **31** 221-6

Hans D, Dargent-Molina P, Schott A M, Sebert J L, Cormier C, Kotzki P O, Delmas P D, Pouilles J M, Breart G and Meunier P J 1996 Ultrasonographic heel measurements to predict hip fracture in elderly women: the EPIDOS prospective study *The Lancet* **348** 511-4

Häusler K D, Rich P A and Barry E B 1997 Water Bath and Contact Methods in Ultrasonic Evaluation of Bone *Calcif. Tissue Int.* **61** 26-9

Hildebrand T, Laib A, Müller R, Dequeker J and Rüegsegger P 1999 Direct Three-Dimensional Morphometric Analysis of Human Cancellous Bone: Microstructural Data from Spine, Femur, Iliac Crest, and Calcaneus *J. Bone Miner. Res.* **14** 1167-74

Hildebrand T and Rüegsegger P 1997 A new method for the model-independent assessment of thickness in three-dimensional images *J. Microsc.* **185** 67-75

Jaworski M, Lebiedowski M, Lorenc R S and Trempe J 1995 Ultrasound bone measurement in pediatric subjects *Calcif. Tissue Int.* **56** 368-71

Johansen A and Stone M 1997 The effect of ankle oedema on bone ultrasound assessment at the heel *Osteoporosis Int.* **7** 44-7

Karlsson M, Duan Y, Ahlborg H, Obrant K, Johnell O and Seeman E 2001 Age, gender, and fragility fractures are associated with differences in quantitative ultrasound independent of bone mineral density *Bone* **28** 118-22

Kaufman J J, Luo G and Siffert R S 2007 A Portable Real-Time Ultrasonic Bone Densitometer *Ultrasound Med. Biol.* **33** 1445-52

Kotzki P O, Buyck D, Hans D, Thomas E, Bonnel F, Favier F, Meunier P J and Rossi M 1994 Influence of fat on ultrasound measurements of the Os calcis *Calcif. Tissue Int.* **54** 91-5

Langton C and Langton D 2000 Comparison of bone mineral density and quantitative ultrasound of the calcaneus: site-matched correlation and discrimination of axial BMD status *The British journal of radiology* **73** 31-5
Langton C M 2011 The 25th anniversary of BUA for the assessment of osteoporosis: Time for a new paradigm? *Proc IMechE, Part H: J Engineering in Medicine* **225** 113-25
Langton C M and Wille M-L 2013 Experimental and computer simulation validation of ultrasound phase interference created by lateral inhomogeneity of transit time in replica bone: marrow composite models *Proc IMechE, Part H: J Engineering in Medicine* **227** 890-5
Langton C M, Wille M-L and Flegg M B 2014 A deconvolution method for deriving the transit time spectrum for ultrasound propagation through cancellous bone replica models *Proc IMechE, Part H: J Engineering in Medicine* **228** 321-9
Le L H 1998 An investigation of pulse-timing techniques for broadband ultrasonic velocity determination in cancellous bone: a simulation study *Phys. Med. Biol.* **43** 2295-308
Lee K I and Choi M J 2007 Phase velocity and normalized broadband ultrasonic attenuation in Polyacetal cuboid bone-mimicking phantoms *J. Acoust. Soc. Am.* **121** EL263-EL9
Lee K I I 2013 Correlations of linear and nonlinear ultrasound parameters with density and microarchitectural parameters in trabecular bone *J. Acoust. Soc. Am.* **134** EL381-EL6
Lees B, Lees B, Stevenson J C and Stevenson J C 1993 Preliminary evaluation of a new ultrasound bone densitometer *Calcif. Tissue Int.* **53** 149-52
Magkos F, Manios Y, Babaroutsi E and Sidossis L S 2005 Quantitative ultrasound calcaneus measurements: normative data for the Greek population *Osteoporosis Int.* **16** 280-8
McCloskey E V, Murray S A, Charlesworth D, Miller C, Fordham J, Clifford K, Atkins R and Kanis J A 1990 Assessment of broadband ultrasound attenuation in the os calcis in vitro *Clinical science (London, England : 1979)* **78** 221-5
McKelvie M L, Fordham J, Clifford C and Palmer S B 1989 In vitro comparison of quantitative computed tomography and broadband ultrasonic attenuation of trabecular bone *Bone* **10** 101-4
Moayyeri A, Adams J E, Adler R A, Krieg M A, Hans D, Compston J and Lewiecki E M 2012 Quantitative ultrasound of the heel and fracture risk assessment: an updated meta-analysis *Osteoporosis Int.* **23** 143-53
Nicholson P H F, Haddaway M J and Davie M W J 1994 The dependence of ultrasonic properties on orientation in human vertebral bone *Phys. Med. Biol.* **39** 1013-24
Njeh C, Hodgskinson R and Langton C 1995 Determination of bone strength from ultrasonic velocity and broadband ultrasound attenuation Br. J. Radiol. **68** 789-96
Njeh C F, Boivin C M and Langton C M 1997 The role of ultrasound in the assessment of osteoporosis: A review *Osteoporosis Int.* **7** 7-22
Njeh C F, Hans D, Li J, Fan B, Fuerst T, He Y Q, Tsuda-Futami E, Lu Y, Wu C Y and Genant H K 2000 Comparison of Six Calcaneal Quantitative Ultrasound Devices: Precision and Hip Fracture Discrimination *Osteoporosis Int.* **11** 1051-62
Padilla F, Jenson F, Bousson V, Peyrin F and Laugier P 2008 Relationships of trabecular bone structure with quantitative ultrasound parameters: In vitro study on human proximal femur using transmission and backscatter measurements *Bone* **42** 1193-202
Prins S H, Jørgensen H L, Jørgensen L V and Hassanger C 1998 The role of quantitative ultrasound in the assessment of bone: a review Clin. Physiol. **18** 3-17
Thompson P W, Taylor J, Oliver R and Fisher A 1998 Quantitative ultrasound (QUS) of the heel predicts wrist and osteoporosis-related fractures in women age 45–75 years *J. Clin. Densitometry* **1** 219-25
Wear K A 2000 The effects of frequency-dependent attenuation and dispersion on sound speed measurements: applications in human trabecular bone *IEEE Transactions on Ultrasonics, Ferroelectrics and Frequency Control* **47** 265-73
Wear K A 2009a The dependencies of phase velocity and dispersion on volume fraction in cancellous-bone-mimicking phantoms *J. Acoust. Soc. Am.* **125** 1197-201
Wear K A 2009b Ultrasonic attenuation in parallel-nylon-wire cancellous-bone-mimicking phantoms *J. Acoust. Soc. Am.* **124** 4042-6
Wille M-L and Langton C M 2016 Solid volume fraction estimation of bone:marrow replica models using ultrasound transit time spectroscopy *Ultrasonics* **65** 329-37
Wille M L, Almualimi M A and Langton C M 2016 Pulse-echo ultrasound transit time spectroscopy: A comparison of experimental measurement and simulation prediction *Proc IMechE, Part H: J Engineering in Medicine* **230** 20-9
Xu Y, Guo B, Gong J, Xu H and Bai Z 2014 The correlation between calcaneus stiffness index calculated by QUS and total body BMD assessed by DXA in Chinese children and adolescents *J. Bone Miner. Metab.* **32** 159-66

Zhang C, Le L H, Zheng R, Ta D and Lou E 2011 Measurements of ultrasonic phase velocities and attenuation of slow waves in cellular aluminum foams as cancellous bone-mimicking phantoms *J. Acoust. Soc. Am.* **129** 3317-26